




## RESEARCH ARTICLE

10.1029/2023SW003601

# Modeling Pipe to Soil Potentials From Geomagnetic Storms in Gas Pipelines in New Zealand

Tim Divett<sup>1</sup> , Malcolm Ingham<sup>1</sup> , Gemma Richardson<sup>2</sup> , Mark Sigley<sup>3</sup>, and Craig J. Rodger<sup>4</sup> 

<sup>1</sup>School of Chemical and Physical Sciences, Victoria University of Wellington, Wellington, New Zealand, <sup>2</sup>British Geological Survey, Edinburgh, UK, <sup>3</sup>First Gas Ltd., New Plymouth, New Zealand, <sup>4</sup>Department of Physics, University of Otago, Dunedin, New Zealand

### Key Points:

- We modeled New Zealand's gas pipeline network to calculate pipe to soil potentials due to uniform electric fields of 100 mV/km
- Potentials are greatest at ends of pipelines, following theoretical curves with variations due to branches and changes in direction
- The lower coating conductance of the branchlines leads to higher potentials on both that line and connected lines

### Correspondence to:

T. Divett,  
[tim.divett@vuw.ac.nz](mailto:tim.divett@vuw.ac.nz)

### Citation:

Divett, T., Ingham, M., Richardson, G., Sigley, M., & Rodger, C. J. (2023). Modeling pipe to soil potentials from geomagnetic storms in gas pipelines in New Zealand. *Space Weather*, 21, e2023SW003601. <https://doi.org/10.1029/2023SW003601>

Received 13 JUN 2023  
Accepted 14 NOV 2023

### Author Contributions:

**Conceptualization:** Tim Divett, Malcolm Ingham, Gemma Richardson, Craig J. Rodger

**Data curation:** Mark Sigley

**Formal analysis:** Tim Divett, Malcolm Ingham

**Funding acquisition:** Craig J. Rodger

**Investigation:** Tim Divett, Malcolm Ingham

**Methodology:** Tim Divett, Gemma Richardson

**Resources:** Malcolm Ingham, Mark Sigley

**Software:** Tim Divett, Gemma Richardson

**Supervision:** Malcolm Ingham

**Visualization:** Tim Divett

**Writing – original draft:** Tim Divett, Malcolm Ingham

**Abstract** Gas pipelines can experience elevated pipe to soil potentials (PSPs) during geomagnetic disturbances due to the induced geoelectric field. Gas pipeline operators use cathodic protection to keep PSPs between  $-0.85$  and  $-1.2$  V to prevent corrosion of the steel pipes and disbondment of the protective coating from the pipes. We have developed a model of the gas pipelines in the North Island of New Zealand to identify whether a hazard exists to these pipelines and how big this hazard is. We used a transmission line representation to model the pipelines and a nodal admittance matrix method to calculate the PSPs at nodes up to 5 km apart along the pipelines. We used this model to calculate PSPs resulting from an idealized  $100$  mVkm<sup>-1</sup> electric field, initially to the north and east. The calculated PSPs are highest at the ends of the pipelines in the direction of the applied electric field vector. The calculated PSP follows a characteristic curve along the length of the pipelines that matches theory, with deviations due to branchlines and changes in pipeline direction. The modeling shows that the PSP magnitudes are sensitive to the branchline coating conductance with higher coating conductances decreasing the PSPs at most locations. Enhanced PSPs produce the highest risk of disbondment and corrosion occurring, and hence this modeling provides insights into the network locations most at risk.

**Plain Language Summary** Steel pipelines are used to transport natural gas across long distances. These pipes are covered in an insulating coating to protect them from corrosion. During a geomagnetic storm, there are rapid changes in Earth's magnetic and electric fields. These changes cause electrical currents to flow through breaks in the insulating coating and on and off the pipelines, resulting in a voltage between Earth and the pipe. Over time the currents can cause corrosion and the voltages can lead to the coating separating from the pipe, resulting in further corrosion. We have developed a model of New Zealand's gas pipeline network and used it to calculate the voltages in the pipelines in New Zealand's North Island during a simplified geomagnetic storm. This model will help us understand where the greatest risk of corrosion is and how widespread the risk is. The highest risk is at the ends of the pipeline, aligned with the direction of the imposed electric field. Branchlines and changes in direction of the pipeline change the local voltages.

## 1. Introduction

It is well known that space weather can effect technological structures on Earth, through the geomagnetic activity associated with solar storms (e.g., Bothmer & Daglis, 2007). When a coronal mass ejection arrives at Earth and interacts with the magnetosphere, the resulting time variations in the geomagnetic field result in induced electric fields in the conducting Earth. The resulting fields can lead to geomagnetically induced currents (GICs) flowing between the ground and any sufficiently long conductor, such as steel pipelines or power transmission lines, and a voltage between these conductors and the soil. The voltage between steel gas pipelines and Earth due to geomagnetic activity is known as telluric pipe to soil potential (PSP) (Boteler & Seager, 1998). The total PSP is a combination of this telluric PSP, arising from geomagnetic activity, and the voltage applied to the pipelines by rectifiers as part of the cathodic protection (CP) system applied by pipeline operators.

FirstGas Ltd. own and operate over 2,500 km of pipelines to distribute natural gas in the North Island of New Zealand. These steel pipelines are coated with an insulating coating and are protected by a CP system, such as described by Ingham et al. (2022), which seeks to hold the pipeline at a potential between  $-0.85$  and  $-1.2$  V relative to Earth. If the potential between the steel pipe and Earth drops below  $-1.2$  V the insulating coating can disbond from the steel pipe, allowing ground water to come into contact with the steel, leading to corrosion (e.g.,

© 2023. The Authors.

This is an open access article under the terms of the [Creative Commons Attribution License](https://creativecommons.org/licenses/by/4.0/), which permits use, distribution and reproduction in any medium, provided the original work is properly cited.

**Writing – review & editing:** Tim Divett, Malcolm Ingham, Gemma Richardson, Mark Sigley, Craig J. Rodger

von Baeckmann et al., 1997). Further, if this potential exceeds  $-0.85$  V for a sufficiently long duration, the pipes may corrode. During normal operation this potential is dominated by the applied rectifier voltage. During strong space weather events, when there may be large variations in induced electric fields high PSPs can occur and the CP system may be unable to protect the pipelines, leading to increased corrosion and the risk of disbondment occurring.

Modeling PSPs in pipelines can help assess the risk to this infrastructure by identifying the magnitude and location of the largest PSPs during severe geomagnetic storms. Modeling can also identify locations where mitigation could help prevent long term corrosion or disbondment. Modeling of PSPs in a single, isolated pipeline has identified that the PSP is highest at the ends of long sections of pipeline parallel to the electric field, with a characteristic PSP curve tending exponentially toward zero in the middle (Boteler & Seager, 1998). Pulkkinen et al. (2001) modeled GICs and PSPs in idealized sections of pipeline and a simplified Finnish pipeline network for a uniform electric field and found similar characteristic curves, with variation around junctions.

A time varying magnetic field induces an electric field in the conducting Earth. In the presence of a pipeline the induced field is modified such that the electric field inside the pipe is not necessarily the same as that away from the pipe. The effect of the pipe can be modeled with the result that for periods of variation above about 10 s the electric field in the pipe is the same as the electric field in the ground. At periods less than 10 s, the electric field in the pipe is increasingly attenuated at higher frequency. Overall, this leads to a potential difference (PSP) between the pipe and the local ground. This calculation assumes an Earth with no variation with depth. The effect of induced electric fields in a more realistic Earth model and for real pipelines or pipeline networks, including bends, branches and discontinuities, can be modeled by distributed-source transmission line (DSTL) theory as developed initially by Dabkowski (1979) and applied to the problem of geomagnetic induction in pipelines by Boteler and Cookson (1986).

Boteler (2013) introduced a more versatile method to calculate PSPs which simplifies the representation of the pipelines by using an equivalent- $\pi$  transmission line representation of the pipeline network, then used the nodal admittance matrix method to calculate GICs. Boteler's (2013) method was used by Lax et al. (2019) to model PSPs in two theoretical pipelines: a straight line, and a pipeline with a junction, a bend and a change in diameter. We have used this versatile method in the present paper to calculate PSPs in the North Island's gas pipeline network. The same matrix method has previously been used to calculate and model GICs in electrical transmission lines in New Zealand (Divett et al., 2017, 2018, 2020; Mac Manus, Rodger, Ingham, et al., 2022; Mukhtar et al., 2020). Rodger et al. (2020), Mukhtar et al. (2020), Mac Manus, Rodger, Dalzell, et al., 2022, and Mac Manus, Rodger, Ingham, et al., 2022 identified a potential for high GICs at the western and eastern ends of the North Island's electrical transmission lines in Taranaki and Hawke's Bay, respectively. Place names are shown in Figure 1.

Observations of GICs and PSPs on New Zealand's gas pipelines have been reported previously by Ingham and Rodger (2018) and Ingham et al. (2022). Ingham et al. (2022) analyzed monitoring data from FirstGas' CP system at several locations in the North Island during geomagnetic storms. Of these observation locations, the largest PSPs were found at the end of the Hawke's Bay branchline. Further, they found considerable differences between the timing of maximum PSP at locations near each other on the same branchline.

In the current study we present the development of a representation of the gas pipeline network in the North Island of New Zealand in Section 2 and also describe how we applied the versatile method developed by Boteler (2013) to calculate the PSPs on these pipelines, given (in the current study) a constant, uniform electric field. In Section 3 we show how these PSPs vary around the pipeline network for two directions of the electric field. In Section 3.3 we show how the PSPs vary with changing electric field direction and five different pipeline coating conductances at sites where observed PSPs were reported by Ingham et al. (2022).

## 2. Modeling Methods

### 2.1. The Electrical Properties of the NZ Gas Pipeline Network

The natural gas transmission pipelines in New Zealand's North Island consist of 2,523 km of high pressure steel pipelines, as shown in Figure 1. The main section of the network runs from the major gas production area in Taranaki, north to Auckland and south to Wellington. Significant branchlines off the main northward

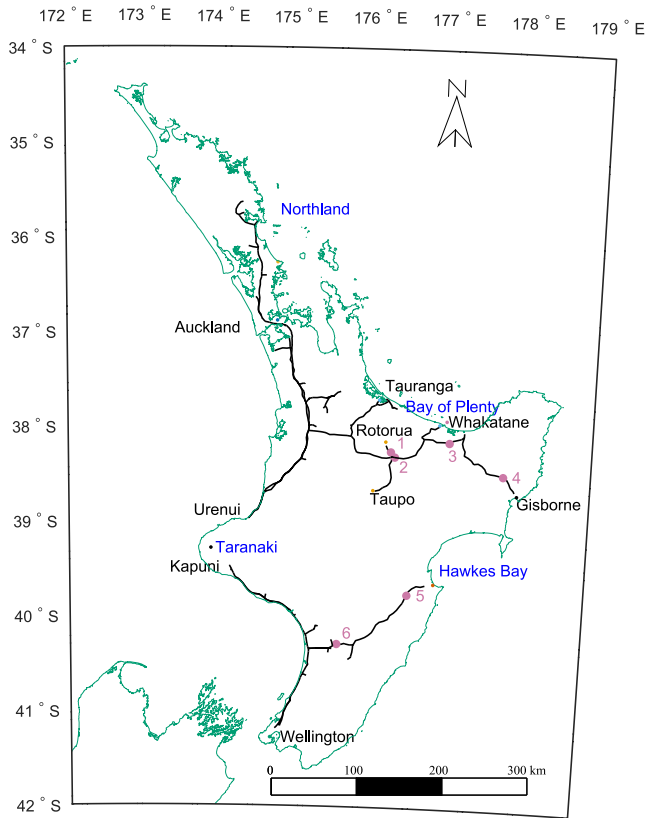


**Figure 1.** The North Island of New Zealand, showing FirstGas Ltd.'s pipelines (in black), numbered observation sites (in magenta), and locations mentioned in the text. Note that the Auckland to Wellington pipeline is electrically isolated at multiple locations in Taranaki, and thus this pipe is shown ending in Urenui and restarting in Kapuni, reflecting the electrical properties of the pipeline.

and southward pipeline sections are seen running northeastward to Hawke's Bay, and eastward to Bay of Plenty (on separate pipeline routes) and north of Auckland to Northland.

A flange on the main section of pipeline electrically isolates the pipelines south of Taranaki from those to the north. Within Taranaki there are substantial zinc earthing connections on the pipeline, in a horseshoe shape around Mount Taranaki (which is located roughly where the word "Taranaki" is shown in Figure 1). Hence the main pipelines running from Taranaki to Wellington, and Taranaki to Auckland are electrically split at Taranaki and thus in the modeling reported here we ignore the pipelines within Taranaki. We have replaced the earthing points and the complex web of pipelines within Taranaki with a single node at Urenui, treated as the southern end of the Auckland to Taranaki line shown in Figure 1.

The pipelines are mostly installed below ground and are coated with a resistive coating to prevent corrosion and increase resistance between the steel pipeline and Earth. The coating is predominantly coal tar enamel on the main pipelines from Taranaki to Wellington and Auckland, while a more modern coating is mostly used on the branchlines. Examples of the modern coatings are two or three layer polyethylene, or fusion bonded epoxy. The pipelines coated with coal tar enamel coating are over 46 years old.

The specific conductance of the coal tar enamel coating is assumed to be  $C_{\text{main}} = 100 \mu\text{Sm}^{-2}$ , while that of the other coatings is assumed to be  $C_{\text{branch}} = 1 \mu\text{Sm}^{-2}$ . These conductances are based on estimates provided by CP engineers working at FirstGas Ltd. and are consistent with the  $5 \mu\text{Sm}^{-2}$  used to represent a "typical modern coating" by Boteler (2013). They both fall within the "excellent" coating quality defined as less than  $100 \mu\text{Sm}^{-2}$  (NACE International, 2002). There is considerable uncertainty in the values reported by NACE International (2002), with a broad range reported in the literature for the conductance of each coating type. This range of values is partly due to the potential for changes in conductance after installation due to damage, soil moisture and salinity, as well as variations in manufacturing. Further, any scratch or defect in the pipeline coating can significantly reduce

the local resistance. In the modeling reported below, to explore the effect of changes in coating conductance we present a sensitivity analysis by applying five values between 1 and  $100 \mu\text{Sm}^{-2}$  to the branchline coating conductance.

The pipeline network is protected from corrosion by impressed current CP as discussed by Ingham et al. (2022). At 48 locations on the network, rectifiers with associated anode beds are used to keep the pipeline at a suitable negative potential with respect to earth. Active monitoring of the PSP and the potential of an installed metal coupon, both with respect to a reference electrode, is carried out at multiple locations with measurements made every second. Six of the locations where observations of the PSPs are made in this way are indicated by numbers in Figure 1.

FirstGas Ltd. provided a shapefile with the location, pipe diameter and wall thickness, and the coating type and thickness for the entire pipeline network. Using these locations, we divided the pipeline into sections, separated by nodes, that are short enough that each section can be assumed to be straight and, if a varying electric field were applied, the electric field could be assumed constant along a section. Most sections are  $L = 5 \text{ km}$  long, except at junctions where  $L$  is the length required to complete the distance from the last node to the node at the junction. Lax et al. (2019) indicate that sections less than 10 km can be considered sufficiently short that they are less than the electrical adjustment distance. The node locations in the shapefile left gaps at most pipeline junctions. Using aerial photos on the websites Google Maps and Land Information New Zealand, we identified that there is above ground gas infrastructure at these locations. FirstGas Ltd. confirmed that almost all of these locations are electrically continuous. They comprise two main types: (a) main line valves and smaller stations with no, or minimal, earthing and no electrical break, (b) larger stations or stations with extensive earthing, which have

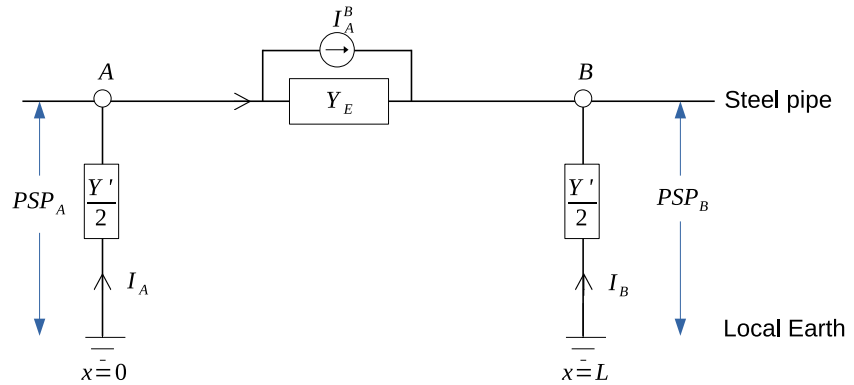


**Figure 2.** The equivalent-pi representation of a section of pipe.

insulating joints and a bond-cable spanning the joint. We therefore manually added connections between nodes at 106 locations to account for this in the model.

The electrical characteristics of each section of pipeline were calculated from information in the shapefile. The admittance to ground,  $Y$ , depends on the coating conductance and the surface area per unit distance, and the series impedance per unit length,  $Z$ , depends on the resistivity of steel and the cross-sectional area of the pipeline steel. We calculated these properties for each section of pipeline using  $Y = C2\pi r_o$ , and  $Z = \frac{\rho}{\pi(r_o^2 - r_i^2)}$ , where  $r_o$  and  $r_i$  are the outer and inner radii of the pipe,  $C$  is the assumed coating conductance, and  $\rho = 0.18 \times 10^{-6} \Omega\text{m}$  is the standard resistivity of steel. While the resistivity of steel is well known, the coating conductance is not and consequently we tested the sensitivity of PSP to coating conductance in Sections 3.1.1 and 3.3.

## 2.2. Spatially Uniform Electric Field

To model pipe to soil potentials on the pipeline, we have applied a spatially uniform electric field,  $E = 100 \text{ mVkm}^{-1}$ , to the whole NZ region in several directions. This is approximately the size of the spatial average of the electric field reported by Ingham et al. (2022) at the peak of a Kp 7+ storm on 28 August 2018. Initially a northward and an eastward field were applied to explore the effects of those electric fields on the gas pipelines. Subsequently, we applied an electric field at directions between  $0^\circ$  and  $350^\circ$  clockwise from north in  $10^\circ$  increments. This was to explore the effects of the full range of electric field directions at six locations where observations of the PSPs are available. We make the standard assumption that GICs and PSPs are direct current (i.e., DC rather than AC), as the frequencies of geoelectric field variation are sufficiently low that we can ignore capacitance.

### 2.2.1. Equivalent-pi Representation

The connection between the steel pipeline and Earth is continuous, through the highly resistive pipeline coating, along the length of the pipeline. Following Boteler (2013) we have used the equivalent-pi transmission line theory to discretize the continuous earthing of the pipelines, as shown in Figure 2. In this way, the continuous connection to Earth is represented by a discrete admittance to ground,

$$\frac{Y'}{2} = \frac{\cosh(\gamma L) - 1}{Z_0 \sinh(\gamma L)}, \quad (1)$$

at each end of each pipeline section. Here  $\gamma = \sqrt{ZY}$  is the propagation constant,  $\frac{1}{\gamma}$  is the adjustment distance, and  $Z_0 = \sqrt{\frac{Z}{Y}}$  is the characteristic impedance of the pipeline section, shown in Table 1. The effect of the electric field between nodes  $A$  and  $B$  is applied as an equivalent current source,

$$I_A^B = \frac{E}{Z}, \quad (2)$$

in parallel with the series admittance of each pipeline section,

$$Y_E = \frac{1}{Z_0 \sinh(\gamma L)}. \quad (3)$$

Pipeline	$C(\mu\text{Sm}^{-2})$	$Z(\Omega \text{ km}^{-1})$	$Y(\text{S km}^{-1})$	$Z_0(\Omega)$	$\gamma(\text{km}^{-1})$	$\frac{1}{\gamma}(\text{km})$
Main	100	0.042 to 0.053	0.06	0.92	0.052 to 0.058	17 to 19
Branch	1	0.01 to 0.38	0.00016 to 0.0014	2.7 to 49	0.0038 to 0.0078	130 to 260

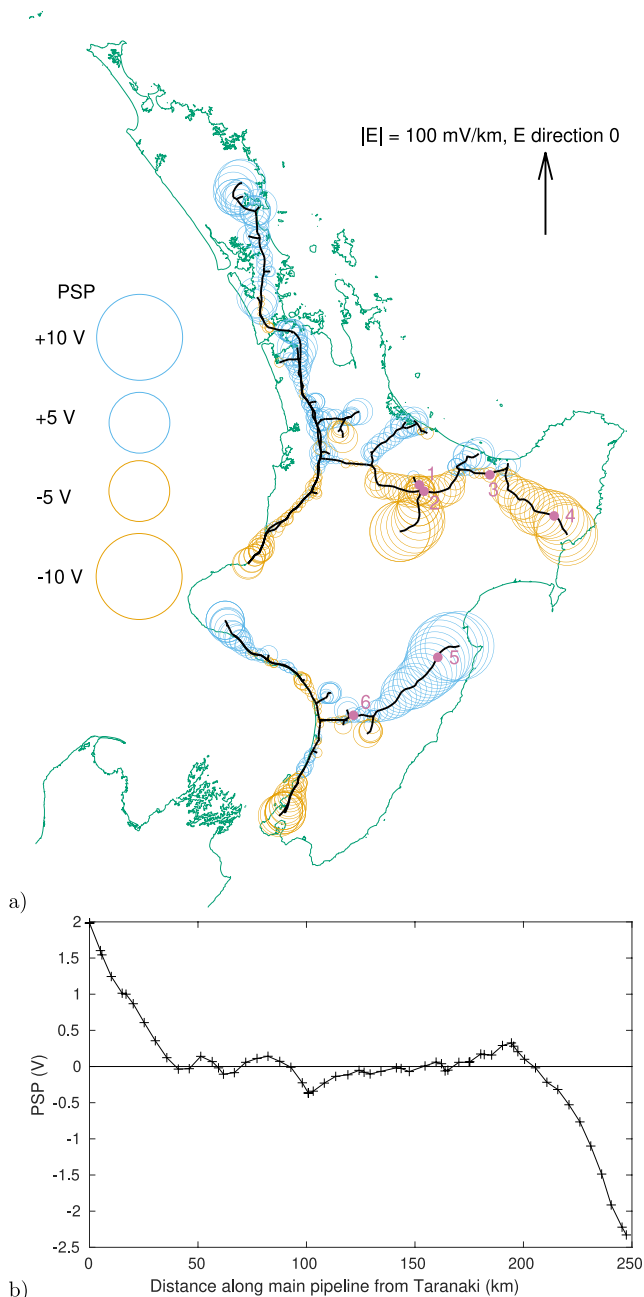


**Figure 3.** PSPs due to a northward electric field. (a) in the whole of the North Island, (b) on the main pipeline from Taranaki to Wellington.

### 2.3. Converting to a Nodal Network and Calculating PSPs

To calculate the currents and PSPs for every node on the pipeline network we combine the equivalent-pi representations for all single pipeline sections into a nodal admittance network, again following Boteler (2013). The first step is to join all pipeline sections that connect at each node. The admittance to ground at that node is then the sum of the admittances of each adjacent pipeline section at that node.

The vector of equivalent current sources at each node,  $[J]$ , is the sum of the equivalent current sources directed into each node. The PSP due to geomagnetic variation at each node on the network can then be calculated by solving the matrix equation

$$[V] = [Y]^{-1}[J] \quad (4)$$

where  $[Y]$  is the admittance matrix, formed by summing the admittance to Earth and the series admittances for all pipelines connected to node  $i$  to give the diagonal components.  $-Y_E$  between nodes  $i$  and  $j$  gives the off-diagonal components.

## 3. Modeling Results

As outlined above, we have modeled PSPs resulting from a uniform  $100 \text{ mVkm}^{-1}$  electric field oriented in a number of different specific directions. In reality PSPs in pipelines are influenced by spatial variations in the electric field, due to variations in geomagnetic field and ground conductivity structure, as well as characteristics of the pipelines. Studying the modeled PSPs due to uniform electric fields is useful for identifying the influence of the topography of the pipeline network on PSPs, in isolation from the other variations. But it is worth remembering that, in reality, both the magnitude and orientation of the induced electric field will vary considerably over even a small area.

### 3.1. PSPs Resulting From a Northward Electric Field

PSPs calculated at each node on the NZ pipeline network in response to a uniform  $100 \text{ mVkm}^{-1}$  northward-directed electric field are shown in Figure 3a. Blue (orange) circles denote positive (negative) PSP, with the size of the circle showing the PSP magnitude. In general, for a northward electric field, positive PSPs are at the northern ends of pipelines while negative PSPs are at the southern ends, as expected. Also as expected, the PSPs are largest at the ends of pipelines, especially the longer north to south pipelines. These trends are developed by GICs flowing on to a pipeline in the south, accumulating along the length of the pipeline to halfway, and flowing to Earth toward the northern ends of the pipelines.

These large-scale trends result in the characteristic PSP curves shown in Figure 3b for the main pipeline from Taranaki to Wellington. The large-scale

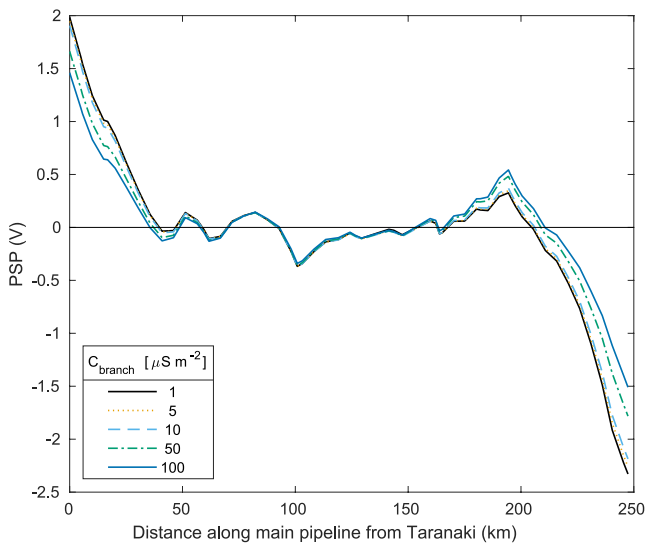


**Figure 4.** Pipe to soil potential along the main pipeline from Taranaki to Wellington for five branchline coating conductances with a northward electric field, for comparison with Figure 3b which shows the case where  $C_{\text{branch}} = 1 \mu\text{Sm}^{-2}$ .  $C_{\text{main}}$  is kept constant at  $100 \mu\text{Sm}^{-2}$ . Note the values for  $C_{\text{branch}} = 1$  to  $10 \mu\text{Sm}^{-2}$  are so similar that the lines are difficult to distinguish.

trends in these curves match the characteristic curves for PSP on a single long, straight pipeline presented by, among others, Boteler and Seager (1998). However, their characteristic curves were for a pipeline that does not contain significant branches or changes in direction. Deviations from those large-scale trends for the main Taranaki to Wellington pipeline are apparent, especially near the middle of this pipeline near where the Hawke's Bay line branches toward the east. On the main line, the maximum PSP is at the northern end, as expected for a northward electric field. Heading south toward Wellington the PSP decreases steadily, apart from a small increase seen 15 km south of Taranaki where a long parallel line connects to the main line, continuing parallel to the south almost to the end of the main line. Continuing southward the next small increase in PSP occurs 50 km south of Taranaki where a short pipeline branches to the north, followed by five small increases associated with pipelines that branch off the main pipeline over the next 150 km.

The largest of these branches is the eastward pipeline which runs off from this branch point to Hawke's Bay. On this branch there is another PSP curve characteristic of a pipeline aligned primarily with the direction of the electric field. The effects of the two characteristic curves are not independent, as the main Taranaki to Wellington line is electrically connected to the Hawke's Bay branchline, allowing GICs to flow through both pipelines. Hence, the PSP around the junction of these two pipelines is affected by the combined effect of the characteristic curves on both pipelines. Further, effects due to the short branch lines are also seen on the Hawke's Bay line near the connection with the main Taranaki to Wellington line.

The same trends shown in the characteristic curve for Taranaki to Wellington are also apparent in the PSPs on the other north-south oriented pipelines to the north of Taranaki in Figure 3a. This is particularly prominent in the main pipeline from Taranaki to Auckland, with the trend continuing north to Northland. Although the trend in PSP is complicated around Auckland and Northland due to parallel pipelines, a large east-west bend and multiple short branchlines, the highest PSPs are still at the northern end of the Northland branchline. The north-south trends are also apparent in the branch lines from Taupo to Tauranga, and Gisbourne to Whakatane. The effects of the short branchlines are also apparent on these lines although not as obvious as south of Taranaki because these lines are more complicated than the pipelines south of Taranaki.

Another interesting feature of the PSP can be seen in the east-west sections within the main north to south pipeline, in Figure 3a. Particularly around Auckland, the PSPs are very small at a location where the pipelines are oriented nearly perpendicular to the direction of the electric field. This is as expected for a pipeline perpendicular to the electric field. However, it is very noticeable at this location where the larger scale trend for the PSP would indicate that PSP should be larger if the pipeline did not change direction. This effect is also noticeable on the east-west oriented sections of the Bay of Plenty branchline, especially at the westernmost end and in the short section near observation site 3.

### 3.1.1. Sensitivity of PSP to Branchline Coating Conductance

There is considerable uncertainty about the value of coating conductance, due to the cumulative effects of exposure to soil moisture and potential damage during installation and operation (Alrudayni, 2015; NACE International, 2002). Further, it is well recognized in the pipeline industry that the lower conductance values of modern pipeline coatings leads to larger telluric PSP variations than on older pipelines with relatively higher coating conductance (e.g., Boteler et al., 1999). Consequently, it is worth exploring the effect of varying conductance on calculated PSPs.

For the modeled PSPs shown in Figure 3 the main Taranaki to Wellington pipeline has a coating conductance of  $100 \mu\text{Sm}^{-2}$ , while the Hawke's Bay branch has a coating conductance of  $1 \mu\text{Sm}^{-2}$ . While it is expected that, for a single pipeline, a higher conductance of the pipeline coating will lead to a reduction in PSP along the length of the pipeline, it is of interest to see how varying the coating conductance of the Hawke's Bay branch affects the PSPs between Taranaki and Wellington. This is shown in Figure 4, again for a northward oriented electric field, which

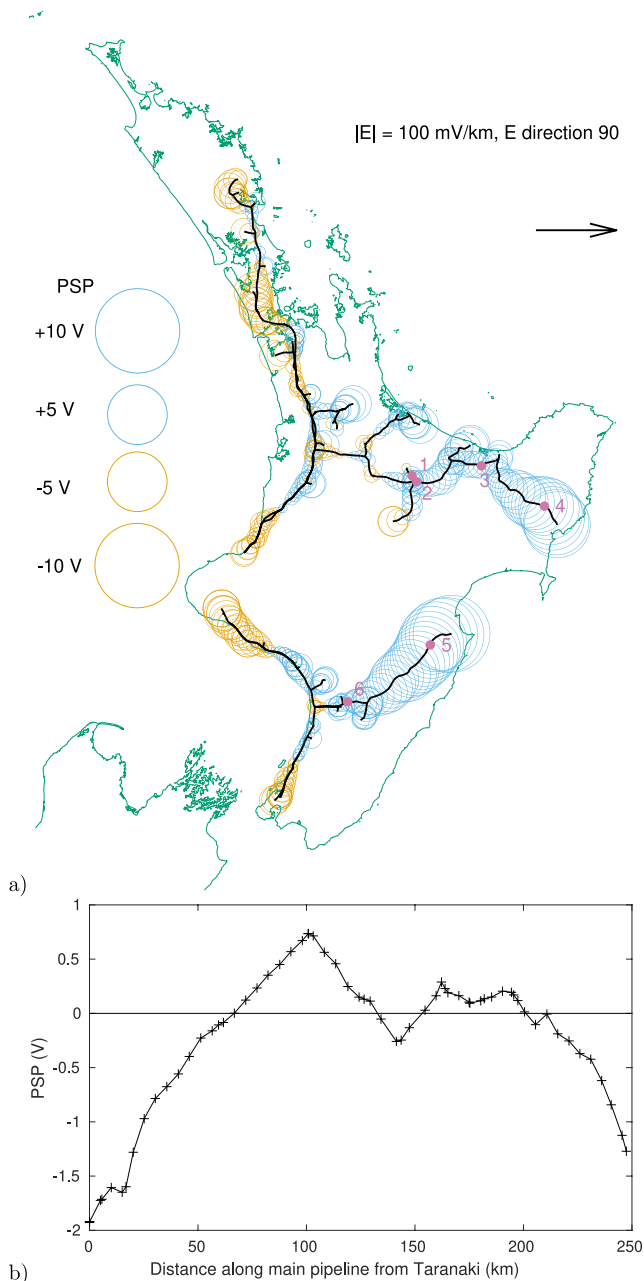


**Figure 5.** PSPs due to an eastward directed electric field. (a) in the whole of the North Island, (b) on the main pipeline from Taranaki to Wellington.

Only the western half of each characteristic curve is on the main line, with the eastern halves on the Hawke's Bay branchline. The first of these curves shows negative PSP in Taranaki and positive PSP some 100 km along the pipeline. The second curve shows positive PSPs from this point onward, gradually becoming negative further south, with a local minimum 144 km from Taranaki at the connection with the Hawke's Bay branchline. This is as expected for an eastward electric field, considering that the most eastward point on this section of the main line is at that 144 km point, and the large impact of the Hawke's Bay branchline, which connects to the main line at the easternmost point on the main line. The Hawke's Bay branchline acts to reduce the PSP on the main line for approximately 20 km either side of the connection with the main line.

shows the calculated PSPs along the Taranaki to Wellington pipeline for five different coating conductances on the Hawke's Bay line. This plot should be compared with Figure 3b, which is the black line shown in Figure 4.

It is apparent from Figure 4 that at both the Taranaki and Wellington ends of the main pipeline increasing the conductance of the Hawke's Bay line coating by a factor of 100 reduces the magnitude of calculated PSP by about 25%. The decrease in PSPs along the majority of the main pipeline results from an increase in current passing on to the Hawke's Bay line from Earth as the resistance of the branchline's coating is decreased. As the two lines are connected, this increased current then contributes to the total current in the Taranaki to Wellington pipeline, thereby lowering the PSPs on the main line. The general shape of the PSP curve from 180 to 250 km in Figure 4 means that the overall decrease in PSP as the coating conductance on the Hawke's Bay line is increased appears as an increase in PSP in the localized region between 180 and 200 km. This location is just to the south of a short eastward branch line to the south of the main Hawke's Bay branch (Figure 1). Replacing the northward electric field with an eastward electric field results in a similar reduction in the magnitude of PSPs by about 25% at most locations on this pipeline. This essentially reinforces the fact that observed PSPs are influenced by the entire pipeline network rather than specific local effects.

### 3.2. PSPs Resulting From an Eastward Electric Field

The PSPs calculated at all nodes on the pipeline network for an eastward  $E$  field of  $100 \text{ mVkm}^{-1}$  are shown in Figure 5a. These PSPs are highest (more positive) in the direction of the tip of the electric field vector, and lowest (more negative) in the opposite direction, in the same manner as the PSPs for a northward electric field. For an eastward directed electric field this means that positive PSPs are seen in the east of the pipeline network while negative PSPs are seen in the west. Again, the greatest magnitude PSPs are at the ends of the pipelines, especially at the eastern ends of the branchlines to Hawke's Bay and Gisbourne. In both cases a single point at the eastern end, so the high eastern PSP is shared between the corresponding negative voltages at the two western ends. The smallest magnitude PSPs occur toward the middle of the lines. These large-scale trends are all consistent with the characteristic PSP curves for single, long, straight pipelines, as discussed previously. There are also deviations from these large scale trends associated with branchlines and changes in direction of the pipelines in a similar way to the PSPs due to a northward  $E$  field.

The variation in PSP with distance along the main line between Taranaki and Wellington is quite different to that for the northward  $E$  field. The variation for an eastward  $E$  field (Figure 5b) appears as two characteristic curves placed end to end. Only the western half of each characteristic curve is on the main line, with the eastern halves on the Hawke's Bay branchline. The first of these curves shows negative PSP in Taranaki and positive PSP some 100 km along the pipeline. The second curve shows positive PSPs from this point onward, gradually becoming negative further south, with a local minimum 144 km from Taranaki at the connection with the Hawke's Bay branchline. This is as expected for an eastward electric field, considering that the most eastward point on this section of the main line is at that 144 km point, and the large impact of the Hawke's Bay branchline, which connects to the main line at the easternmost point on the main line. The Hawke's Bay branchline acts to reduce the PSP on the main line for approximately 20 km either side of the connection with the main line.

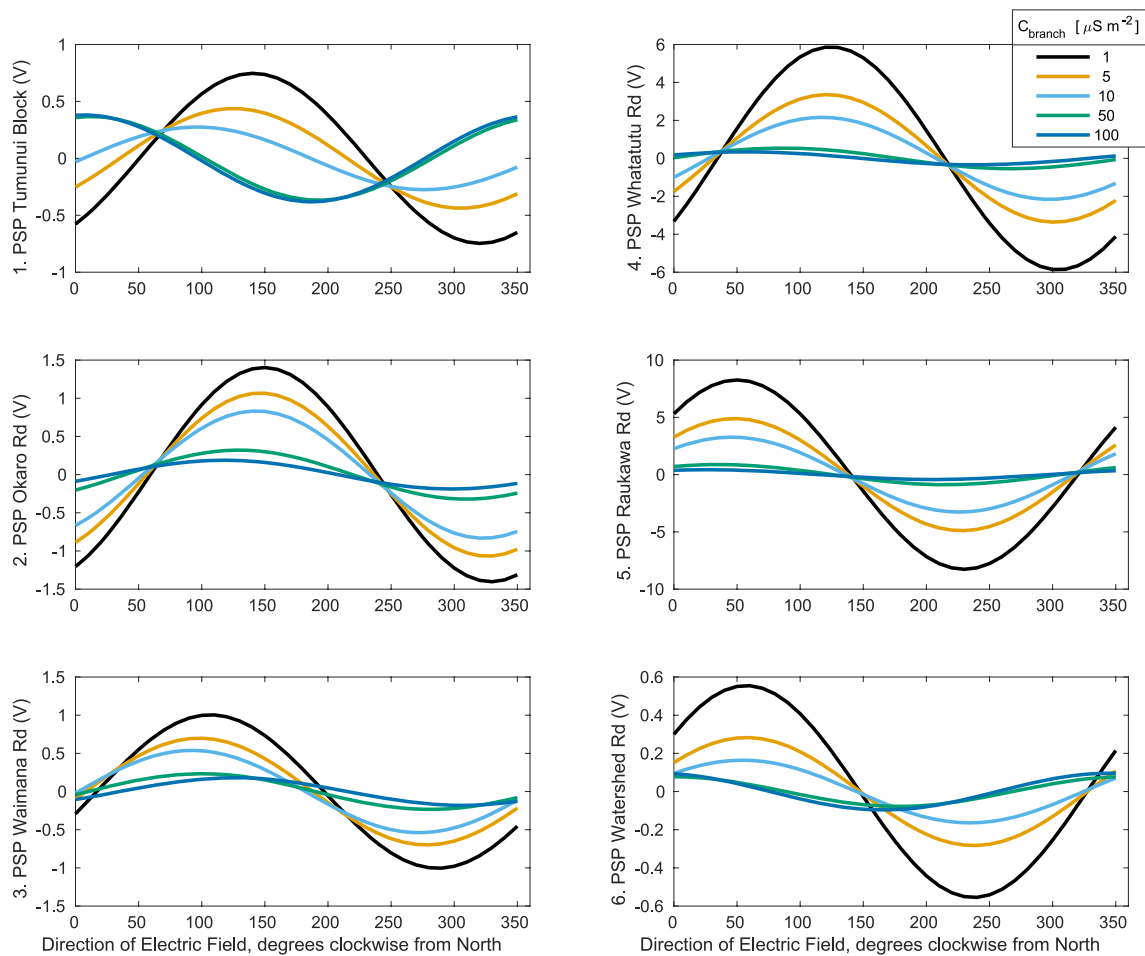


**Figure 6.** Pipe to soil potential at six observation sites for five modern branchline coating conductances.  $C_{main}$  is kept constant at  $100 \mu\text{Sm}^{-2}$ .

### 3.3. PSPs at Observation Locations

The variation in calculated PSPs at 6 locations on the pipeline network as the direction of the electric field changes are shown in Figure 6. The location of each site is marked by magenta numbers in Figure 1. For five values of the branchline pipeline coating conductance, each of these figures shows a sinusoidal response in PSP as the electric field changes direction between  $0$  and  $350^\circ$  clockwise from north. The lowest conductance in these figures ( $C_{branch} = 1 \mu\text{Sm}^{-2}$ , shown in black) corresponds to that used in the previous sections, and represents FirstGas' best estimate of the actual branchline coating conductance.  $C_{main}$  is kept constant at  $100 \mu\text{Sm}^{-2}$ . That conductance results in the largest PSPs for all directions of electric field, at all sites.

The two greatest magnitudes of modeled PSP are at sites 4 and 5, respectively. The PSPs at these sites reduce with increasing branchline conductance. PSPs at these sites are up to an order of magnitude higher than the other observation sites. This is primarily due to these sites being close to the ends of the long branchlines to Gisborne and Hawke's Bay, respectively. However, the directions of the electric field at which these maximums occur,  $120^\circ$  and  $50^\circ$  respectively, does not vary with coating conductance. These are the directions for which the electric fields are roughly parallel to the overall direction of the pipelines ending near these sites. Previously, Ingham and Rodger (2018) found that measured telluric currents at one location on the Hawke's Bay branchline were associated with electric fields perpendicular to that section of pipeline, concluding that the PSP at a given location is due to the electric field over the whole pipeline network. The results from the current study are consistent with Ingham and Rodger's (2018) conclusion.

In contrast, at the other four sites, the electric field orientation which gives maximum PSP does depend on  $C_{branch}$ . This is seen as a slight decrease in the  $E$  field angle which gives maximum PSP at sites 2, but a much more



significant and obvious dependence at sites 1, 3, and 6. This changing direction of electric field giving peak PSP with  $C_{\text{branch}}$  shows that the PSP at locations away from the ends of pipeline sections is sensitive to a combination of the direction of  $E$  relative to the pipeline direction, and the electrical conductivity of the pipeline coating.

PSPs at sites 1, 2, 3 and 6 also show a general decrease in magnitude with increasing  $C_{\text{branch}}$ , in the same manner as for sites 4 and 5. However, at site 1 PSP is larger for  $C_{\text{branch}} = 100 \mu\text{Sm}^{-2}$  than for  $C_{\text{branch}} = 50 \mu\text{Sm}^{-2}$ . At site 6 near the junction of the main line and the Hawke's Bay branchline, the PSP is lower than at most other sites due to the site's position near the center of the southern pipeline network. The PSP is a combination of those from each of the two lines. The contribution to the PSP from the main Taranaki to Wellington line does not change with  $C_{\text{branch}}$  while the contribution from the branchline does. While the direction from Wellington to Taranaki on the main line is just west of north, the Hawke's Bay line is oriented to the northeast. Consequently the maximum contribution to PSP at site 6 will be aligned with these respective directions. The direction of  $E$  that results in maximum PSP for different branchline conductances is thus due to the relative contribution to PSP from the branchline and the main line.

#### 4. Discussion

The calculated PSPs in the current study are not only comparable with those reported in previous studies such as Trichtchenko and Boteler (2002), Boteler (2013), and Pulkkinen et al. (2001), but also with the range of monitoring data reported by Ingham et al. (2022). Ingham et al. (2022) found that, of the sites discussed in Section 3.3, site 5 had the largest PSPs of these sites during a storm on 28 August 2018 (site 4 was not reported for this disturbance). The observed PSPs of up to 8 V compare favorably with the modeled PSPs for higher values of  $C_{\text{branch}}$ . The electric field of  $100 \text{mVkm}^{-1}$  used in the present study is also close to the spatial average at the time of maximum  $B_x$  during that storm, although the orientation of the induced electric field was certainly not uniform and was mostly oriented to the northwest (Ingham et al., 2022), almost perpendicular to the local orientation of the pipeline.

We have shown that the lower coating conductance of modern pipeline coatings leads to higher PSPs, compared to older coal tar enamel coating. Although this might at first sight seem counter-intuitive, it must be remembered that coatings are designed without regard to space weather but with the aim of insulating the pipeline from Earth. Modern coatings also provide a better barrier to corrodents in the environment and to the flow of the electrical component of electrochemical corrosion cells (von Baeckmann et al., 1997).

The large scale patterns of highest magnitude PSPs at the ends of pipeline, with smaller PSPs in the middle of the network, match the results of calculations of GICs in electrical transmission lines in the North Island reported by Rodger et al. (2020), Mukhtar et al. (2020), and Mac Manus, Rodger, Ingham, et al., 2022. Similar results have been found by Beggan et al. (2013), Blake et al. (2016), Bailey et al. (2018), and Divett et al. (2018) for the UK, Ireland, Austria and the South Island of New Zealand, respectively.

#### 5. Summary

We have modeled PSPs in the gas pipelines in New Zealand's North Island using a nodal matrix method to calculate voltages and currents in a transmission line representation of the pipelines. We applied a uniform electric field of  $100 \text{mVkm}^{-1}$  to explore the effect of, initially, a northward and eastward electric field on the PSP along these pipelines. The highest PSPs are at the ends of the pipelines, with positive PSPs at the end of the pipeline corresponding to the tip of the electric field vector and negative PSPs toward the tail. The trend in PSP along the length of the main pipeline between Wellington and Taranaki follows the characteristic curves presented by Boteler and Seager (1998) and Boteler (2013). Deviations from these trends occur near connections to branchlines, changes in pipeline direction, and connections to parallel pipelines.

Increasing the coating conductance of the branchlines decreases the magnitude of the PSPs on the main line from Taranaki to Wellington. Increasing this conductance also decreases the magnitude of PSP near the ends of branchlines to Hawke's Bay and Bay of Plenty. We have also investigated the electric field direction at which the maximum PSP occurs at six sites on the pipeline network. The direction of this maximum is generally aligned with the overall direction of the pipeline leading to and from each site. There is a change in this direction of  $E$  for maximum PSP at some sites close to the junction between the main line and branch lines.

The model of PSPs in New Zealand's gas pipeline developed in this paper is part of a staged development approach to modeling the effect of an extreme geomagnetic storm. In future work we plan to develop this model further to explore the effect of a spatially and temporally varying electric field due to ground conductance and the varying magnetic field during a real geomagnetic storm and a simulated extreme storm. We also plan to add the earthing electrodes in northern Taranaki and explore the effects of installing ground beds at suitable locations to investigate their role in reducing PSPs. We note that this staged approach to building a representative network model, informed by simultaneous examination and analysis of electrical monitoring observational data has proved very successful for GIC modeling in the New Zealand electrical transmission network. In particular, it has led to the production of a validated model to examine GIC in the power transmission network, allowing investigation of extreme geomagnetic storm scenarios and informed mitigation planning (Mac Manus, 2023; Mac Manus, Rodger, Dalzell, et al., 2022; Mac Manus, Rodger, Ingham, et al., 2022). As a detailed real-world example of a pipeline model that calculates PSPs for space weather purposes this study will also hopefully be useful as a benchmark study elsewhere.

### Data Availability Statement

Information about pipeline properties used here are the property of First Gas New Zealand Ltd. Request for access to this information should be addressed in the first instance to Mark Sigley ([mark.sigley@firstgas.co.nz](mailto:mark.sigley@firstgas.co.nz)).

### References

- Alrudayni, M. A. (2015). Evaluation of external coating performance on buried pipelines in the oil and gas industry. (Master of Science, Florida International University). <https://doi.org/10.25148/etd.FIDC000143>
- Bailey, R. L., Halbedell, T. S., Schattauer, I., Achleitner, G., & Leonhardt, R. (2018). Validating GIC models with measurements in Austria: Evaluation of accuracy and sensitivity to input parameters. *Space Weather*, 16(7), 887–902. <https://doi.org/10.1029/2018SW001842>
- Beggan, C. D., Beamish, D., Richards, A., Kelly, G. S., & Thomson, A. W. P. (2013). Prediction of extreme geomagnetically induced currents in the UK high voltage network. *Space Weather*, 11(7), 407–419. <https://doi.org/10.1002/swe.20065>
- Blake, S. P., Gallagher, P. T., McCauley, J., Jones, A. G., Hogg, C., Campagna, J., et al. (2016). Geomagnetically induced currents in the Irish power network during geomagnetic storms. *Space Weather*, 14(12), 1136–1154. <https://doi.org/10.1002/2016sw001534>
- Boteler, D. H. (2013). A new versatile method for modelling geomagnetic induction in pipelines. *Geophysical Journal International*, 193(1), 98–109. <https://doi.org/10.1093/516gji/ggs113>
- Boteler, D. H., & Cookson, M. (1986). Telluric currents and their effects on pipelines in the Cook Strait region of New Zealand. *Materials Performance*, 25(3), 27–32.
- Boteler, D. H., Gummow, R., & Rix, B. (1999). Evaluation of telluric current effects on the maritimes and northeast pipeline. In *Proceedings, NACE northern area eastern conference, Ottawa* (pp. 1–13).
- Boteler, D. H., & Seager, W. H. (1998). Telluric currents: A meeting of theory and observation. *Corrosion*, 54(9), 751–755. <https://doi.org/10.5006/1.3284894>
- Bothmer, V., & Daglis, I. A. (2007). *Space weather- physics and effects*. Springer Berlin Heidelberg. <https://doi.org/10.1007/522978-3-540-34578-7>
- Dabkowski, J., & Taflove, A. (1979). Power engineering society for presentation at the IEEE Transactions on Power Apparatus and Systems, PAS (Vol. 98(3), pp. 788–794). <https://doi.org/10.1109/tpas.1979.319291>
- Divett, T., Ingham, M., Beggan, C. D., Richardson, G. S., Rodger, C. J., Thomson, A. W. P., & Dalzell, M. (2017). Modeling geoelectric fields and geomagnetically induced currents around New Zealand to explore GIC in the South Island's electrical transmission network. *Space Weather*, 15(10), 1396–1412. <https://doi.org/10.1002/2017SW001697>
- Divett, T., Mac Manus, D. H., Richardson, G. S., Beggan, C. D., Rodger, C. J., Ingham, M., et al. (2020). Geomagnetically induced current model validation from New Zealand's South Island. *Space Weather*, 18(8), e2020SW002494. <https://doi.org/10.1029/2020SW002494>
- Divett, T., Richardson, G. S., Beggan, C. D., Rodger, C. J., Boteler, D. H., Ingham, M., et al. (2018). Transformer-level modeling of geomagnetically induced currents in New Zealand's South Island. *Space Weather*, 16(6), 718–735. <https://doi.org/10.1029/2018SW001814>
- Ingham, M., Divett, T., Rodger, C. J., & Sigley, M. (2022). Impacts of GIC on the New Zealand gas pipeline network. *Space Weather*, 20(12), e2022SW003298. <https://doi.org/10.1029/2022SW003298>
- Ingham, M., & Rodger, C. J. (2018). Telluric field variations as drivers of variations in cathodic protection potential on a natural gas pipeline in New Zealand. *Space Weather*, 16(9), 1396–1409. <https://doi.org/10.1029/2018SW001985>
- Lax, K., Boteler, D. H., Charalambous, C. A., & Pirjola, R. (2019). Practical application of telluric modelling for pipelines. In *European federation of corrosion* (pp. 1–11). Retrieved from <http://eurocorr.efcwweb.org/2019/abstracts/55016/179136.pdf>
- Mac Manus, D. H. (2023). *Geomagnetically induced currents: Validating observations and modelling in New Zealand*. PhD thesis, University of Otago. Retrieved from <https://ourarchive.otago.ac.nz/handle/10523/154>
- Mac Manus, D. H., Rodger, C. J., Dalzell, M., Renton, A., Richardson, G. S., Petersen, T., & Clilverd, M. A. (2022). Geomagnetically induced current modeling in New Zealand: Extreme storm analysis using multiple disturbance scenarios and industry provided hazard magnitudes. *Space Weather*, 20(12), e2022SW003320. <https://doi.org/10.1029/2022SW003320>
- Mac Manus, D. H., Rodger, C. J., Ingham, M., Clilverd, M. A., Dalzell, M., Divett, T., & Petersen, T. (2022). Geomagnetically induced current model in New Zealand across multiple disturbances: Validation and extension to NonMonitored transformers. *Space Weather*, 20(2), e2021SW002955. <https://doi.org/10.1029/2021SW002955>
- Mukhtar, K., Ingham, M., Rodger, C. J., Mac Manus, D. H., Divett, T., Heise, W., et al. (2020). Calculation of GIC in the North Island of New Zealand using MT data and thin-sheet modeling. *Space Weather*, 18(11), e2020SW002580. <https://doi.org/10.1029/2020SW002580>
- NACE International (2002). *NACE standard TM 0102-2002 standard test method measurement of protective coating electrical conductance on underground pipelines*. NACE International The Corrosion Society.
- Pulkkinen, A., Pirjola, R., Boteler, D., Viljanen, A., & Yegorov, I. (2001). Modelling of space weather effects on pipelines. *Journal of Applied Geophysics*, 48(4), 233–256. [https://doi.org/10.1016/S0926-9851\(01\)00109-4](https://doi.org/10.1016/S0926-9851(01)00109-4)

- Rodger, C. J., Clilverd, M. A., Mac Manus, D. H., Martin, I., Dalzell, M., Brundell, J. B., et al. (2020). Geomagnetically induced currents and harmonic distortion: Storm-time observations from New Zealand. *Space Weather*, *18*(3), 1–20. <https://doi.org/10.1029/2019SW002387>
- Trichtchenko, L., & Boteler, D. H. (2002). Modelling of geomagnetic induction in pipelines. *Annales Geophysicae*, *20*(7), 1063–1072. <https://doi.org/10.5194/angeo-20-1063-2002>
- von Baeckmann, W., Schwenk, W., & Prinz, W. (1997). *Handbook of cathodic corrosion protection*. Elsevier. Retrieved from <http://www.science-direct.com/science/article/pii/B9780884150565500162>